Eur. Phys. J. C 49, 91–96 (2007)
DOI 10.1140/epjc/s10052-006-0071-z

THE EUROPEAN PHYSICAL JOURNAL C

Regular Article – Theoretical Physics

Studying the energy dependence of elliptic and directed flow within a relativistic transport approach

H. Petersen[a], M. Bleicher

Institut für Theoretische Physik, Johann Wolfgang Goethe-Universität, Max-von-Laue-Str. 1, 60438 Frankfurt am Main, Germany

Received: 28 July 2006 /
Published online: 22 November 2006 –

Abstract. The energy excitation functions of directed flow (v_1) and elliptic flow (v_2) from $E_{\rm beam} = 90\,A\,$MeV to $E_{\rm cm} = 200\,A\,$GeV are explored within the UrQMD framework and discussed in the context of the available data. The radial and the elliptic flow of the particles produced in a relativistic heavy-ion collision are intimately connected to the pressure and its gradients in the early stage of the reaction. Therefore, these observables should also be sensitive to changes in the equation of state. To prove this connection, the temporal evolution of the pressure, pressure gradients and elliptic flow are shown. For the flow excitation functions it is found that, in the energy regime below $E_{\rm beam} \leq 10\,A\,$GeV, the inclusion of nuclear potentials is necessary to describe the data. Above 40 $A\,$GeV beam energy, the UrQMD model starts to underestimate the elliptic flow. Around the same energy the slope of the rapidity spectra of the proton directed flow develops negative values. This effect is known as the third flow component ("antiflow") and cannot be reproduced by the transport model. The difference between the data and the UrQMD model can possibly be explained by assuming a phase transition from hadron gas to quark–gluon plasma around $E_{\rm lab} = 40\,A\,$GeV. This would be consistent with the model calculations, indicating a transition from hadronic matter to "string matter" in this energy range. Thus, we speculate that the missing pressure might be generated by strong interactions in the early pre-hadronic/partonic phase of central Au + Au (Pb + Pb) collisions already at lower SPS energies.

PACS. 25.75.-q; 25.75.Ld; 25.75.Dw; 25.75.Gz; 24.10.Lx

1 Introduction

It is a major goal of the current and future study of high energy heavy-ion collisions to create extremely hot and dense matter with partons as its fundamental components [1]. This new state of matter is called the quark–gluon plasma (QGP) and is expected to be very similar to the situation in the early universe. However, due to the complex nature of the relativistic nucleus–nucleus reactions, the QGP, if it has been created, escapes direct detection. Therefore, in order to establish the existence and later on to investigate the properties of the new state of matter, one must find observables which allow one to deduce the properties of the intermediate (QGP) state from the final state hadrons.

The exploration of the transverse collective flow is the earliest predicted observable to probe heated and compressed nuclear matter. The transverse flow is intimately connected to the pressure gradients. Therefore, it is sensitive to the equation of state (EoS) and might be used to search for abnormal matter states and phase transitions [2–4].

The intermediate energy regime available at CERN-SPS or at the future GSI-FAIR facility is often referred to as the right place to look for a phase transition to the QGP. Lattice QCD (lQCD) calculations [5, 6] show that the critical temperature is around 170 MeV (for $\mu_b = 0$) and the critical energy density is around 1 GeV/fm^3. This value can already be reached at 20–30 $A\,$GeV beam energy. At finite baryo-chemical potential, the heated and compressed nuclear matter created at these energies crosses the phase transition line possibly even on the high μ side of the critical endpoint. Therefore, it is possible to talk about a phase transition of first order, here. During such a first order phase transition the softest point in the equation of state would be mostly pronounced. For example, the anti-flow around midrapidity ("third flow component"[7]) and the collapse of the elliptic flow observable have been declared as a signal for the phase transition [8, 9].

2 The UrQMD model

For our investigation, the ultra-relativistic quantum molecular dynamics model (UrQMD v2.2) [10, 11] is ap-

[a] e-mail: petersen@th.physik.uni-frankfurt.de

plied to study heavy-ion reactions from $E_{\rm beam} = 90\,A$ MeV to $\sqrt{s_{NN}} = 200$ GeV.The UrQMD model is a relativistic transport model that employs hadronic and string degrees of freedom. It takes into account the formation and multiple scattering of ingoing and newly produced hadrons. It describes dynamically the generation of pressure in the hadronic/valence quark compression and expansion phase. Until now, only hadrons, valence quarks and valence diquarks and their interactions are treated explicitly in this model. Gluonic degrees of freedom are not treated explicitly, but are implicitly present in strings. The UrQMD model reproduces the nucleon–nucleon, meson–nucleon and meson–meson cross section data in a wide kinematic range. It allows for a systematic study of the change in the dynamics from elementary collisions to proton–nucleus and nucleus–nucleus reactions in a unique way without change in the parameters. One advantage of the model for the calculation of the flow observables is the known event plane.

3 Directed flow

The first coefficient of the Fourier expansion of the azimuthal distribution of the emitted particles describes the directed in-plane flow. The directed flow measures the total amount of transverse flow. This flow component is most pronounced in semi-central interactions around target and projectile rapidities where the spectators are deflected away from the beam axis due to a bounce-off from the compressed and heated matter in the overlap region.

To characterize the amount and the direction of the directed flow over the energy range from 2–160 A GeV one can extract the slope around midrapidity from the normalized rapidity distributions usually referred to as the "F" parameter [12]. Normalized means in this case $y/y_{\rm b}$ where $y_{\rm b}$ is the beam rapidity. This normalization accounts for the trivial energy dependence of the slope. The values for the slope in Fig. 1 have been extracted via a polynomial fit of the form $ax + bx^3$ with $x = y/y_{\rm b}$. At low energies, one observes that the inclusion of a nuclear potential is needed to reproduce the data. Here we also show the calculations with inclusion of a mean field from a hard equation of state with momentum dependence and medium-modified nucleon–nucleon cross sections (HMw) [14, 15]. At higher energies the calculations have been performed in the cascade mode without the additional nuclear potentials.

At SPS energies the data develops even negative values for the slope around midrapidity [8, 9]. This behaviour cannot be reproduced within the transport model calculation in cascade mode. However, ideal hydro calculations have predicted the appearance of a so-called "third flow component" [7] or "antiflow" [16] at finite impact parameters. In these analyses it was pointed out that this "antiflow" develops if the matter undergoes a first order phase transition to the QGP. In contrast, a hadronic EoS without QGP phase transition did not yield such an exotic "antiflow" (negative slope) wiggle in the proton flow $v_1(y)$ at low energies.

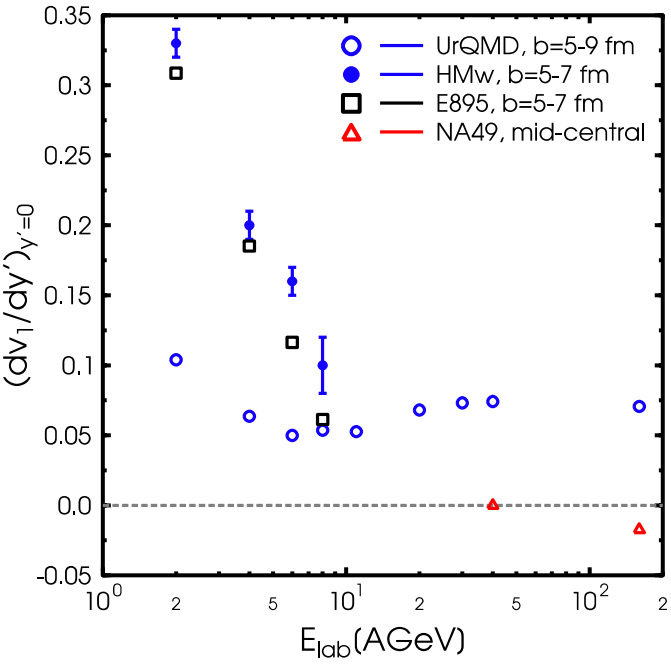

Fig. 1. Slope of $v_1(y)$ of protons around midrapidity extracted from normalized ($y' = y/y_{\rm b}$) rapidity distributions. The data are taken from E895 (*squares*) [12] and NA49 (*triangles*) [13]. UrQMD calculations with included mean field (HMw) are depicted with *full circles*. *Open circles* depict the UrQMD calculation in the cascade mode

4 Elliptic flow

The second coefficient of the Fourier expansion of the azimuthal distribution of the emitted particles (v_2) is called elliptic flow [7, 16–25]. This type of flow is strongest around central rapidities in semi-peripheral collisions. It is driven by the anisotropy of the pressure **gradients**, due to the geometric anisotropy of the initial overlapping region. Therefore, it is a valuable tool to gain insight into the expanding stage of the fire ball. v_2 is defined by

$$v_2 \equiv \langle \cos[2(\phi - \Phi_{\rm RP})] \rangle \,, \tag{1}$$

with $\Phi_{\rm RP}$ being the reaction plane.

4.1 Time evolution

Figures 2 (top) and 3 (top) show the time evolution of the pressure during a heavy-ion collision. The pressure is calculated in a central cell using the kinetic definition:

$$P_{x,y} = \frac{1}{V} \sum_{\rm particles}^{\rm all} \frac{p_{x,y}^2}{E} \tag{2}$$

and

$$P = \frac{1}{2}(P_x + P_y) \,, \tag{3}$$

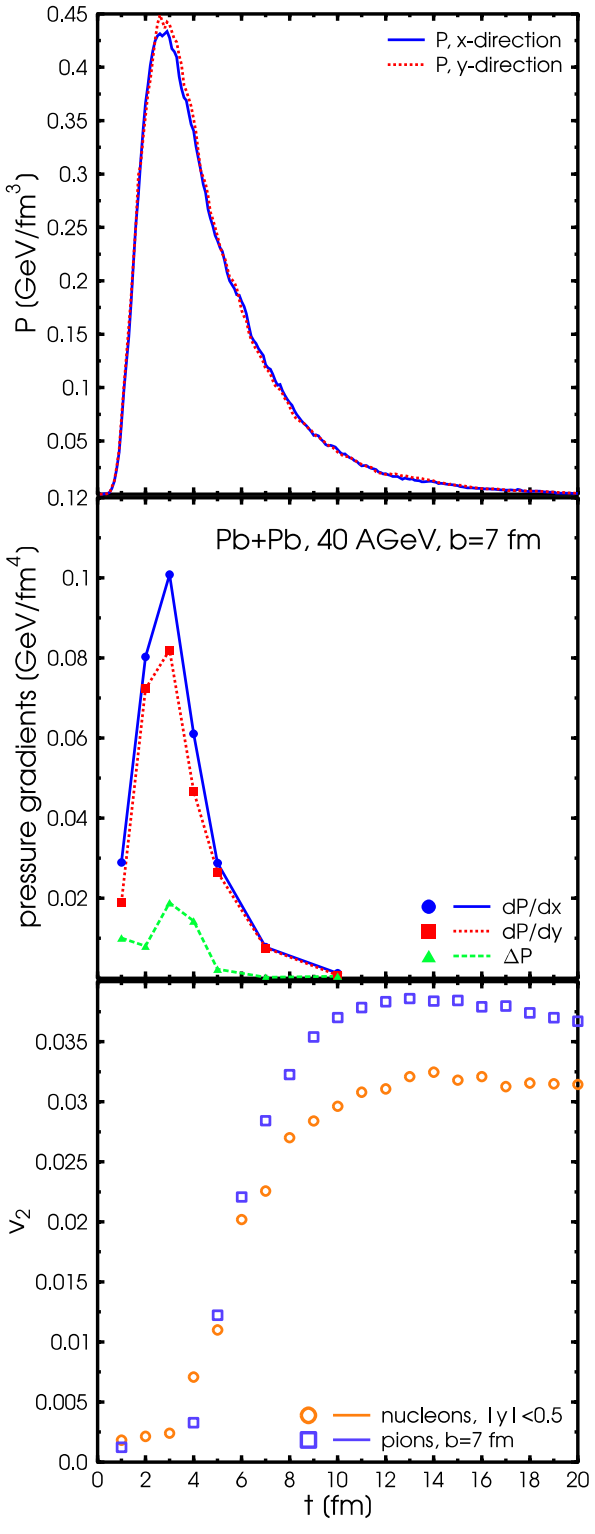

Fig. 2. UrQMD calculation for the time evolution of the pressure; the pressure gradients and elliptic flow for Pb + Pb interactions at $E_{\rm lab} = 40$ A GeV and mid-central collisions ($b = 7$ fm) are shown. *Top*: the kinetic pressure of the interacting particles in the x-direction (*full line*) and in the y-direction (*dotted line*) are displayed. *Middle*: $\mathrm{d}P/\mathrm{d}x$ (*full line*), $\mathrm{d}P/\mathrm{d}y$ (*dotted line*) and the difference between these two , ΔP (*dashed line*), are depicted. *Bottom*: the elliptic flow of pions (*squares*) and nucleons (*circles*) versus time at midrapidity is calculated

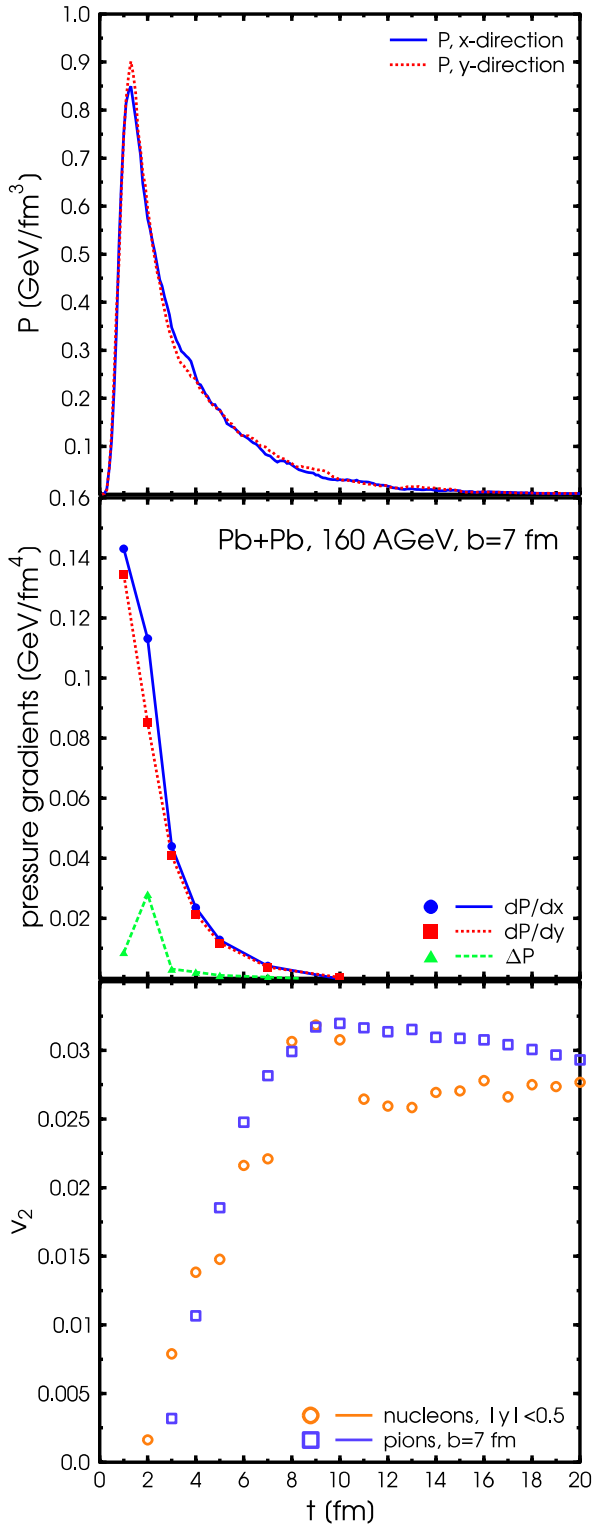

Fig. 3. UrQMD calculation for the time evolution of the pressure; the pressure gradients and elliptic flow for Pb + Pb interactions at $E_{\rm lab} = 160$ A GeV and mid-central collisions ($b = 7$ fm) are shown. *Top*: the kinetic pressure in the x-direction (*full line*) and in the y-direction (*dotted line*) are displayed. *Middle*: $\mathrm{d}P/\mathrm{d}x$ (*full line*), $\mathrm{d}P/\mathrm{d}y$ (*dotted line*) and the difference between these two, ΔP (*dashed line*), are depicted. *Bottom*: the elliptic flow of pions (*squares*) and nucleons (*circles*) versus time at midrapidity is calculated

with $p_{x,y}$ the momentum in the corresponding direction and V is the volume of the cell. With respect to the symmetry of the system the central cell is chosen to be a cylinder with radius $r = 3$ fm and length $h = 3/\gamma_{\rm CM}$ fm. For the calculation of the pressure only particles which interact are taken into account. In UrQMD v2.2 the particles which are produced in string fragmentation get a formation time. During this time only the leading quarks are allowed to interact with a reduced cross section. Therefore most of the particles do not interact until they are "formed" (see also Sect. 4.2).

The absolute pressure values in the transverse directions are almost equal. In Figs. 2 (top) and 3 (top) there can be seen one clear maximum of the pressure which is related to the collision geometry and corresponds to the time of the largest overlap of the two nuclei. This maximum is shifted to earlier times at the higher energy because the collision process is faster.

Let us now explore the time evolution of the pressure gradients in connection to the elliptic flow development. The transverse pressure gradients have been calculated for the first 10 fm at $E_{\rm lab} = 40\ A$ GeV (see Fig. 2 (middle)) and the highest SPS energy (see Fig. 3 (middle)). In both cases one observes large pressure gradients in the very early stage of the collision. For the lower energy the maximum is reached around $t = 3$ fm and for the higher energy it is shifted to even earlier times. The difference between the pressure gradients in x- and y-direction is responsible for the v_2 development. As it can be seen in Figs. 2 (bottom) and 3 (bottom), the temporal evolution of elliptic flow for nucleons and pions starts exactly after this maximum. The elliptic flow increases during the first 6 fm/c, until it reaches almost its final value. After $t = 10$ fm/c it decreases a little because of resonance decays. So, elliptic flow builds up in the early stage of the collision due to the difference of pressure gradients as it is expected.

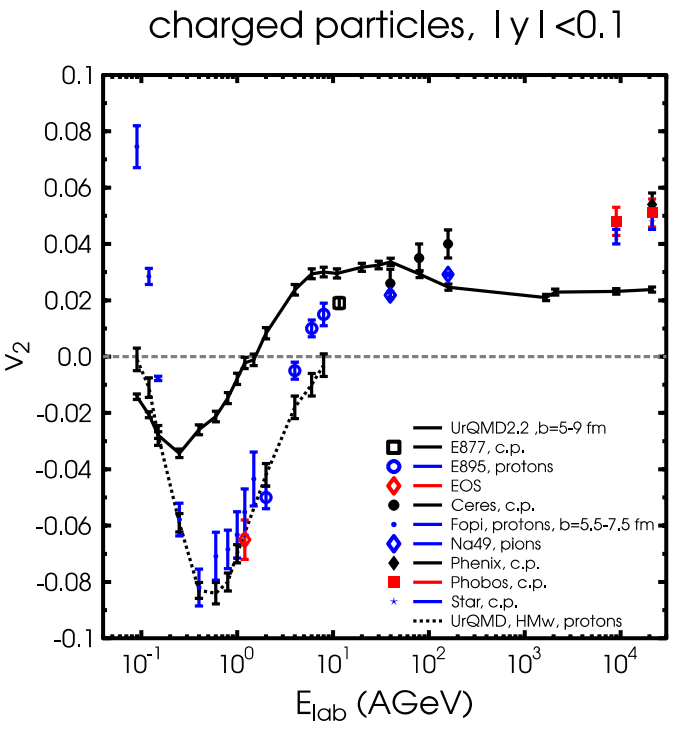

Fig. 4. The calculated energy excitation function of elliptic flow of charged particles in Au + Au/Pb + Pb collisions in mid-central collisions ($b = 5$–9 fm) with $|y| < 0.1$ (*black line*). This *curve* is compared to the data from different experiments for mid-central collisions. For E895 [26, 27] and FOPI [28] there is the elliptic flow of protons and for NA49 [13] it is the elliptic flow of pions. For E877, CERES [29–31], PHENIX [32], PHOBOS [33] and STAR [34] there are data for the charged particle flow. The *dotted line* in the low energy regime depicts UrQMD calculations with the mean field [15]

4.2 Excitation functions

There are two competing effects which lead to contributions with different signs to the integrated v_2 value. At low energies or early times there is the so-called "squeeze-out" effect. The spectator matter blocks the emission in the impact parameter direction and therefore the flowing matter is "squeezed"-out perpendicularly to the reaction plane. This leads to negative elliptic flow values. The second effect is the so-called in-plane flow. This type of flow becomes important at higher energies and/or later times. At higher bombarding energies ($E_{\rm lab} \geq 10\ A$ GeV) the spectators leave the interaction zone quickly. The remaining hot and dense matter expands almost freely, where the surface is such that in-plane emission is preferred. Therefore the elliptic flow receives a positive contribution.

The excitation function of charged particle elliptic flow is compared to the data over a wide energy range (Fig. 4), i.e from $E_{\rm beam} = 90\ A$ MeV to $\sqrt{s_{NN}} = 200$ GeV. The squeeze-out effect at low energies and the change to in-plane emission at higher energies is nicely observed in the excitation function. The symbols indicate the data for charged particles from different experiments. Note however, that in the low energy regime there are only experimental data points for protons. For beam energies below 2 A GeV most of the charged particles are also protons because there is not enough energy to produce many new particles. Going to higher energies the elliptic flow of pions and charged particles are very similar. The rapidity cut of $|y| < 0.1$ has been used for the whole energy range despite the fact that the data at higher energies is within $|y| < 0.5$. This has been done to avoid too much changes in the parameters and this choice gives reasonable results over the whole energy range. We have checked that the results at higher energies are not affected by the choice of this narrower rapidity window.

At low energies $E_{\rm beam} \sim 0.1$–$6\ A$ GeV the squeeze-out effect, i.e. the elliptic flow out-of-plane, is clearly seen in the data as well as in the calculations, especially when the mean field is considered. At such energies, it is well known that both the mean field and the two-body collisions are equally important to reproduce quantitatively the experimental results [35–38]. In this paper we adopt a hard equation of state with a momentum dependence (HMw) which was updated recently in the UrQMD model [14, 15].

In the SPS regime the model calculations are quite in line with the data, especially with the NA49 results. For a more detailed comparison of directed and elliptic flow results from UrQMD-2.2 and NA49 data the reader is referred to [39]. Above $E_{\rm lab} = 160\ A$ GeV the calculation underestimates the elliptic flow. At the highest RHIC energy there is about 5% flow in the data while the model calculation provides only half of this value. This can be explained by assuming a lack of pressure in the transport model at these energies.

It is possible that above the energy range about $E_{\rm lab} = 40\ A$ GeV partonic interactions have to be taken into account to describe the data as suggested in [40–42]. How can we analyse this question in the model, since there are no partonic degrees of freedom explicitly incorporated? In the current model exists a formation time for hadrons produced in the string fragmentation. The leading hadrons of the fragmenting strings contain the valence quarks of the original excited hadron. These (di-) quark string ends are allowed to interact during their formation time with a reduced cross section defined by the additive quark model. Other "pre-hadrons" from the fragmenting string are not allowed to interact before the coalescence of the produced quarks. Thus, because the unformed hadrons do not interact with others during their formation time, the effective pressure is reduced and only build up from the density of the formed hadrons. To illuminate this, we have calculated the energy density during heavy-ion collisions at different beam energies. From this, we extract the time corresponding to the maximum value of the total energy density. Figure 5 shows the fraction of the energy density that is deposited in the "unformed hadrons" ($\epsilon_{\rm partonic}/(\epsilon_{\rm partonic} + \epsilon_{\rm hadronic})$). That is, all string fragments within their formation time are dubbed as 'partonic'. The fraction of $\epsilon_{\rm partonic}$ starts at zero for low energies and then rises fast to almost 100%. Note that this fraction reaches 90% already around 40 A GeV beam energy, similar to the energy region where a phase transition is expected. As one can see, the energy density of the formed hadrons ($\epsilon_{\rm hadronic}$) is much smaller than the total value, therefore the effective pressure of the formed hadrons alone in the model seems to be too small to generate enough v_2. Thus, this finding supports the interpretation of the need for initial pressure from "pre-QGP" matter already at low SPS energies.

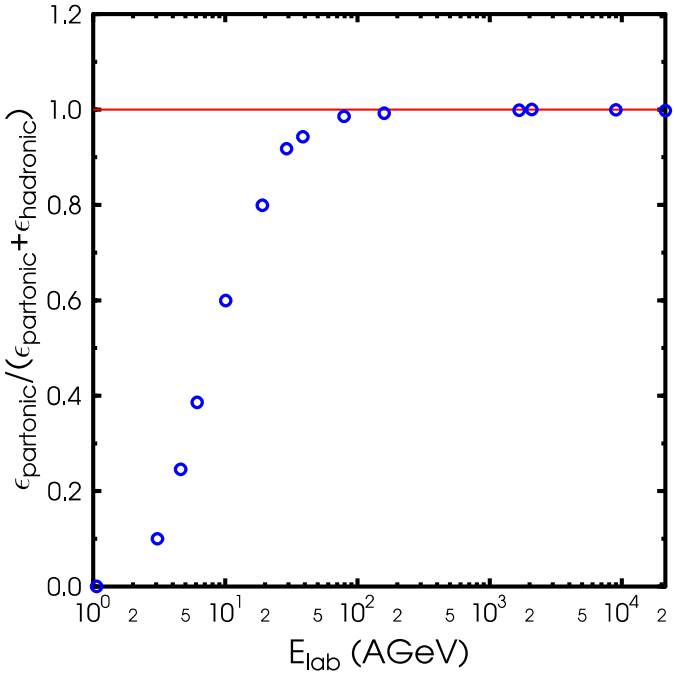

Fig. 5. Calculated fraction of the energy density in unformed hadrons with $|y| < 0.5$ and in a cylindrical volume with transverse radius $r = 3$ fm and length $h = 3/\gamma_{\rm CM}$ fm as a function of the beam energy for central Pb + Pb (Au + Au) reactions

5 Conclusion

We have studied the energy excitation functions of directed and elliptic flow within the UrQMD transport approach and discussed it in the context of the available data. The slope around midrapidity of the rapidity distributions of proton directed flow becomes negative around $E_{\rm lab} = 40\ A$ GeV. This cannot be reproduced by the transport model calculations. The excitation function of elliptic flow shows strong negative flow at low energies – the "squeeze-out" effect – which can quantitatively only be reproduced by including a nuclear potential in the calculation. At high energies we observed an underestimation of the elliptic flow of charged particles in the present model. This can possibly be explained by assuming a lack of pressure in the early stage of the collisions at high energies.

Acknowledgements. We are grateful to the Center for the Scientific Computing (CSC) at Frankfurt for the computing resources. The authors thank the organizers for a great conference. This work was supported by BMBF, DFG and GSI.

References

1. See Proceedings of Quark Matter 2005, Budapest, Hungary, 2005
2. H. Stöcker, J.A. Maruhn, W. Greiner, Z. Phys. A **290**, 297 (1979)
3. J. Hofmann, H. Stöcker, U.W. Heinz, W. Scheid, W. Greiner, Phys. Rev. Lett. **36**, 88 (1976)
4. H. Stöcker, W. Greiner, Phys. Rep. **137**, 277 (1986)
5. Z. Fodor, S.D. Katz, JHEP **0203**, 014 (2002) [arXiv:hep-lat/0106002]
6. Z. Fodor, S.D. Katz, K.K. Szabo, Phys. Lett. B **568**, 73 (2003) [arXiv:hep-lat/0208078]
7. L.P. Csernai, D. Rohrich, Phys. Lett. B **458**, 454 (1999) [arXiv:nucl-th/9908034]
8. H. Stöcker, Nucl. Phys. A **750**, 121 (2005) [arXiv:nucl-th/0406018]
9. H. Stöcker, E.L. Bratkovskaya, M. Bleicher, S. Soff, X. Zhu, J. Phys. G **31**, S929 (2005) [arXiv:nucl-th/0412022]
10. M. Bleicher et al., J. Phys. G **25**, 1859 (1999) [arXiv:hep-ph/9909407]

11. S.A. Bass et al., Prog. Part. Nucl. Phys. **41**, 225 (1998) [arXiv:nucl-th/9803035]
12. E895 Collaboration, H. Liu et al., Phys. Rev. Lett. **84**, 5488 (2000) [arXiv:nucl-ex/0005005]
13. NA49 Collaboration, C. Alt et al., Phys. Rev. C **68**, 034 903 (2003) [arXiv:nucl-ex/0303001]
14. Q.F. Li, Z.X. Li, S. Soff, M. Bleicher, H. Stöcker, J. Phys. G **32**, 151 (2006)
15. Q.F. Li, Z.X. Li, S. Soff, M. Bleicher, H. Stöcker, J. Phys. G **32**, 407 (2006) [arXiv:nucl-th/0601047]
16. J. Brachmann et al., Phys. Rev. C **61**, 024 909 (2000) [arXiv:nucl-th/9908010]
17. H. Sorge, Phys. Rev. Lett. **82**, 2048 (1999) [arXiv:nucl-th/9812057]
18. J.Y. Ollitrault, Phys. Rev. D **46**, 229 (1992)
19. C.M. Hung, E.V. Shuryak, Phys. Rev. Lett. **75**, 4003 (1995) [arXiv:hep-ph/9412360]
20. D.H. Rischke, Nucl. Phys. A **610**, 88C (1996) [arXiv:nucl-th/9608024]
21. H. Sorge, Phys. Rev. Lett. **78**, 2309 (1997) [arXiv:nucl-th/9610026]
22. H. Heiselberg, A.M. Levy, Phys. Rev. C **59**, 2716 (1999) [arXiv:nucl-th/9812034]
23. J. Brachmann, A. Dumitru, H. Stöcker, W. Greiner, Eur. Phys. J. A **8**, 549 (2000) [arXiv:nucl-th/9912014]
24. B. Zhang, M. Gyulassy, C.M. Ko, Phys. Lett. B **455**, 45 (1999) [arXiv:nucl-th/9902016]
25. M. Bleicher, H. Stöcker, Phys. Lett. B **526**, 309 (2002) [arXiv:hep-ph/0006147]
26. E895 Collaboration, C. Pinkenburg et al., prepared for Centennial Celebration and Meeting of the American Physical Society (Combining Annual APS General Meeting and the Joint Meeting of the APS and the AAPT), Atlanta, Georgia, 20–26 March 1999
27. E895 Collaboration, P. Chung et al., Phys. Rev. C **66**, 021 901 (2002) [arXiv:nucl-ex/0112002]
28. FOPI Collaboration, A. Andronic et al., Phys. Lett. B **612**, 173 (2005) [arXiv:nucl-ex/0411024]
29. CERES/NA45 Collaboration, K. Filimonov et al., arXiv: nucl-ex/0109017
30. CERES/NA45 Collaboration, J. Slivova, Nucl. Phys. A **715**, 615 (2003) [arXiv:nucl-ex/0212013]
31. S.I. Esumi, J. Slivova, J. Milosevic for CERES Collaboration SFIN, year XV, Series A: Conferences, No. A2(2002)
32. PHENIX Collaboration, S. Esumi, Nucl. Phys. A **715**, 599 (2003) [arXiv:nucl-ex/0210012]
33. PHOBOS Collaboration, S. Manly et al., Nucl. Phys. A **715**, 611 (2003) [arXiv:nucl-ex/0210036]
34. STAR Collaboration, R.L. Ray, Nucl. Phys. A **715**, 45 (2003) [arXiv:nucl-ex/0211030]
35. P. Danielewicz, Nucl. Phys. A **661**, 82 (1999) [arXiv:nucl-th/9907098]
36. P. Danielewicz, R.A. Lacey, P.B. Gossiaux, C. Pinkenburg, P. Chung, J.M. Alexander, R.L. McGrath, Phys. Rev. Lett. **81**, 2438 (1998) [arXiv:nucl-th/9803047]
37. Q.B. Pan, P. Danielewicz, Phys. Rev. Lett. **70**, 2062 (1993)
38. Q.B. Pan, P. Danielewicz, Phys. Rev. Lett. **70**, 3523 (1993) Erratum
39. H. Petersen, Q. Li, X. Zhu, M. Bleicher, Directed and elliptic flow in heavy-ion collisions at GSI-FAIR and arXiv:hep-ph/0608189
40. E.L. Bratkovskaya et al., Phys. Rev. C **69**, 054 907 (2004) [arXiv:nucl-th/0402026]
41. H. Weber et al., Phys. Lett. B **442**, 443 (1998) [arXiv:nucl-th/9808021]
42. X. Zhu, H. Petersen, M. Bleicher, AIP Conf. Proc. **828**, 17 (2006)